Princeton Plasma Physics Laboratory

PPPL-4061

PPPL-4061

On the Transition from Thermally-driven to Ponderomotively-driven Stimulated Brillouin Scattering and Filamentation of Light in Plasma

R.L. Berger, E.J. Valeo, and S. Brunner

April 2005

Prepared for the U.S. Department of Energy under Contract DE-AC02-76CH03073.

PPPL Report Disclaimers

Full Legal Disclaimer

Trademark Disclaimer

PPPL Report Availability

This report is posted on the U.S. Department of Energy's Princeton Plasma Physics Laboratory Publications and Reports web site in Fiscal Year 2005. The home page for PPPL Reports and Publications is: http://www.pppl.gov/pub_report/

Office of Scientific and Technical Information (OSTI):

Available electronically at: http://www.osti.gov/bridge.

Available for a processing fee to U.S. Department of Energy and its contractors, in paper from:

U.S. Department of Energy
Office of Scientific and Technical Information
P.O. Box 62
Oak Ridge, TN 37831-0062

Telephone: (865) 576-8401

Fax: (865) 576-5728

E-mail: reports@adonis.osti.gov

National Technical Information Service (NTIS):

This report is available for sale to the general public from:

U.S. Department of Commerce
National Technical Information Service
5285 Port Royal Road
Springfield, VA 22161

Telephone: (800) 553-6847

Fax: (703) 605-6900

Email: orders@ntis.fedworld.gov

Online ordering: http://www.ntis.gov/ordering.htm

On the Transition from Thermally-driven to Ponderomotively-driven Stimulated Brillouin Scattering and Filamentation of Light in Plasma

R. L. Berger*

University of California, Lawrence Livermore National Laboratory,

P. O. Box 808, Livermore, CA 94551

E. J. Valeo

Princeton Plasma Physics Laboratory, Princeton, NJ 08540

S. Brunner

Centre de Recherche en Physique des Plasmas,

Association EURATOM-Confédération Suisse,

EPFL, CH-1015, Lausanne, Switzerland

(Dated: 27 February 2005)

Abstract

The dispersion properties of ion acoustic waves and their nonlinear coupling to light waves through ponderomotive and thermal forces are sensitive to the strength of electron-ion collisions. Here, we consider the growth rate of stimulated Brillouin scattering when the driven acoustic wave frequency and wavelength span the range of small to large compared to electron-ion collision frequency and mean free path respectively. We find in all cases the thermal contributions to the SBS growth rate are insignificant if the ion acoustic wave frequency is greater than the electron-ion collision frequency and the wavelength is much shorter than the electron-ion mean free path. On the other hand, the purely growing filamentation instability remains thermally driven for shorter wavelengths than SBS even when the growth rate is larger than the acoustic frequency.

PACS numbers: 52.35.-g, 52.38.-r, 52.57.-z

*Electronic address: berger5@llnl.gov

I. INTRODUCTION

The theory of stimulated Brillouin scatter (SBS) and filamentation in high-temperature, low-Z, and low-density plasma, that is collisionless plasma, has a complete description in terms of Maxwell's equations and the linearized Vlasov equation [1, 2]. If linearized hydrodynamic equations that include inverse bremsstrahlung heating in the electron energy equation use classical Spitzer-H*ä*rm conduction [3], the temperature perturbation contribution to the pressure force in laser produced plasma is typically small compared with the ponderomotive force in the electron momentum equation. [4] However, it has been long recognized [5, 6] that the conditions of applicability for this classical transport, namely, that the electron-electron, λ_{ee} and electron-ion, λ_{ei}, mean free paths be less than the scale length of the temperature perturbation, are often not satisfied. When they are not, the heat conduction is less than the classical value and the temperature perturbations are greater than the classical value. The significance of this increased pressure force to the growth of filaments was recognized by Epperlein [7] who showed that the pressure gradient could dominate the ponderomotive force even if $k\lambda_{ei} > 1$ where k is the wavenumber of the ion acoustic wave. In that work, the electron heat flow is treated as independent of time but as a nonlocal function of x/λ_e, where $\lambda_e \sim \sqrt{\lambda_{ei}\lambda_{ee}}$ is the slowing down mean free path. Subsequent work by Epperlein and others applied and improved on this approach to treat filamentation, forward and backward SBS, and other parametric instabilities that drive ion acoustic waves.

In all this work, it is important to the derivation of the transport coefficients that the frequency and growth rate of the instability be small compared with the electron-ion collision frequency, ν_{ei}. Here, we take a different approach by allowing the complex ion acoustic wave frequency to take on arbitrary values with respect to ν_{ei} to find the SBS and filamentation growth rate for any $k\lambda_{ei}$. We find that thermally-driven SBS is insignificant compared to ponderomotively-driven SBS provided both $k\lambda_{ei} \gg 1$ and $\Re\omega > \nu_{ei}$ where ν_{ei} is the electron-ion collision frequency. For small angle scatter of light, filamentation and forward SBS are two distinct branches of the same dispersion relation. However, filamentation may remain predominantly thermally driven for wavenumbers where forward SBS is predominantly ponderomotively driven.

Epperlein [7] found an effective thermal conductivity as a function of $k\lambda_e$ which is less than the Spitzer-H*ä*rm conductivity when $k\lambda_e \gtrsim 1$ by fitting the time asymptotic steady

state response of a Fokker-Planck code to a sinusoidal spatial modulation of the laser electric field. The conductivity deduced is used in the linearized hydrodynamic equations in place of the Spitzer-Härm conductivity. Large enhancement in the filamentation growth rate above the ponderomotive rate was obtained under conditions when the Spitzer-Härm conductivity would predict no thermal effects. Subsequently, this approach, albeit with somewhat different models for the thermal conductivity, was applied to stimulated Brillouin backscatter by Short and Epperlein [8] and Rose and DuBois [9]. They demonstrated that the coupling of the light to ion acoustic waves is enhanced. In an attempt to find a hydrodynamic formulation valid both when a nonlocal heat conductivity is appropriate and the collisionless limit where Landau damping of the ion acoustic waves can be represented with a Hammet-Perkins conductivity [10], Kaiser [11] proposed an *ad hoc* interpolation between these two approaches with an arbitrary cross over when $k\lambda_e \sim \sqrt{Z}$.

In related work, the damping of ion acoustic waves was found by solving the linearized Fokker-Planck equation that included electron-ion collisions but not electron-electron collisions. The electron-ion collisions are retained in lowest order with a Lorentz operator where an expansion in Legendre polynomials, P_l, is convenient. In the diffusive limit where expansion is truncated after the $l = 1$ coefficient, Bell [12] found an enhancement of the damping above the fluid result for $k\lambda_{ei} \gtrsim .01$. For short wavelengths $k\lambda_{ei} \gtrsim 1$, the damping falls below the collisionless value because Landau damping is precluded by assumption. Epperlein [13] generalized this work by keeping higher order polynomials to obtain the electron damping of ion acoustic waves for arbitrary $k\lambda_{ei}$ and $|\omega|/\nu_{ei}$ where k and ω are the wave's real wavenumber and complex frequency. He found that the damping consisted of a collisionally reduced Landau damping and a collisional (thermal diffusion) damping that involve electrons in distinct regions of velocity space. The diffusive damping is done by electrons that diffuse a wavelength in an oscillation period, $\tau \sim \omega^{-1}$.[12] That is, Landau damping is done by electrons with parallel velocity near the acoustic phase velocity, $v_\parallel = k \cdot v/v \sim \omega/k << v_e$ whereas diffusive damping is done by higher velocity electrons with velocity, $v_\parallel \sim v_e(k\lambda_{ei})^{-1/5}$.

Electron-electron collisions affect the damping for wavenumbers, k, in the intermediate region between the collisional and collisionless limits ($1 < k\lambda_{ei} < 100$) [14] because they drive perturbed distribution function to a more Maxwell-Boltzmann shape. For a given $k\lambda_{ei}$, then, electron self-collisions drive the damping towards the fluid result, and, because

self collisions are more frequent in low Z plasmas, $\nu_{ee} \sim \nu_{ei}/Z$, the damping in low Z plasmas is more fluid-like than high Z plasmas for a given electron-ion collision rate. In another important contribution to a general theory of stimulated scattering from ion waves, Brantov, *et al.* [15] expanded in a Legendre polynomial series the linearized Fokker-Planck equation where both ponderomotive forces as well as inverse bremsstrahlung heating and transport were included through the electron-ion and electron-electron collision operators given a transversely-polarized, high-frequency ($\omega_0 \gg \omega_{pe}$) electromagnetic field. In deriving generalized transport coefficients that included the effects of the high frequency fields, the limit that $|\omega|/\nu_{ei} < 1$ was again invoked. This work allowed the theory of filamentation and SBS [19] in weakly collisional plasma to be developed with a firm theoretical basis with results in substantial agreement with Epperlein [7].

Here, we build on this work by keeping the frequency of the ion waves for all Legendre polynomial coefficients and find the growth rate for filamentation and for backward and forward SBS. In the next Section II, we derive the general dispersion relation. In Section III, the dispersion relation is solved for backward SBS. Section IV and V consider forward SBS and filamentation respectively followed by a discussion of the results in Section VI. The Appendix concerns the inclusion of high order Legendre coefficients in the solution for the lowest two coefficients for the perturbed distribution function.

II. DERIVATION OF GENERALIZED DISPERSION EQUATION FOR STIMULATED SCATTERING

The electron distribution, f, is expanded according to,

$$f = F_0 + \delta f, \tag{1}$$

where $F_0 = (2\pi)^{-3/2} N_{0e} exp(-m_e v^2/T_e)$, an isotropic Maxwellian with density N_{0e} and temperature T_e, satisfies the lowest order equation that defines the equilibrium state about which the system is perturbed by first order electric fields, $\mathbf{E}$, and flows, $\mathbf{u}$. The evolution of the perturbed distribution function (in the frame oscillating with ions) is governed by the equation,

$$\begin{aligned}\left(\frac{\partial}{\partial t} + \mathbf{v}\cdot\nabla\right)\delta f \; - \; & \left(\frac{e}{m_e}\mathbf{E} + \frac{\partial \mathbf{u}}{\partial \mathbf{t}}\right)\cdot\frac{\partial}{\partial v}F_0 - \frac{\partial}{\partial x_\alpha}u_\beta v_\alpha \frac{\partial}{\partial v_\beta}F_0 \\ & = C_{ei}\left(\delta f, F_i\right) + C_{ee}\left(\delta f\right) + S^{nl},\end{aligned} \tag{2}$$

where the linearized electron-electron collision operator is

$$C_{ee}\left(\delta f\right) \;=\; C_{ee}\left(\delta f, F_0\right) + C_{ee}\left(F_0, \delta f\right).$$

In Eq. (2), $\mathbf{v}$ is the electron velocity, e is the electron charge, m_e is the electron mass, C_{ei} is the linearized electron-ion Landau collision operator, and S^{nl} are the terms coupling the electrons to the light waves through the ponderomotive force and inverse bremsstrahlung heating.

Because the collisions between electrons and ions depends only on the relative velocity between species, the form of the ion distribution, F_i, is not important. In light of the dominance of electron-ion collisions, we consider the Fokker-Planck equation for the electrons in which the self-collisions are kept only in the equation for lowest order term in the Legendre polynomial decomposition of the angular dependence of the perturbed distribution but the collisions from the ions are kept to all orders in this decomposition. The linearized kinetic equations have been derived in Reference[15] in which the perturbed electron distribution, δf, is Fourier transformed in time and space and expanded in Legendre polynomials, P_l with coefficients, $f_l(k, w, v)$. The Legendre expansion exploits the fact that these polynomials are eigenfunctions of the Lorentz collision operator. In Ref. [15], however, the acoustic wave frequency was considered small compared with the electron-ion collision frequency in the equations for f_l with $l \geq 1$. Here, we follow the approach of [13] and keep the complex mode frequency ω to all orders. Thus, to the equations (A1) for f_l of Reference [15], we add the term $-i\omega f_l$ to obtain,

$$-i\omega f_0 + i\frac{kv}{3} f_1 \;=\; C_{ee}(f_0) + S_0^{lin} + S_0^{nl}, \tag{3}$$

$$-i\omega f_1 + ikv f_0 + i\frac{2kv}{5} f_2 \;=\; -\nu_1 f_1 + S_1^{lin} + S_1^{nl}, \tag{4}$$

$$-i\omega f_2 + i\frac{2kv}{3} f_1 + i\frac{3kv}{7} f_3 \;=\; -\nu_2 f_2 + S_2^{lin} + S_2^{nl}, \tag{5}$$

$$-i\omega f_3 + i\frac{3kv}{5} f_2 + i\frac{4kv}{9} f_4 \;=\; -\nu_3 f_3 + S_3^{nl}, \tag{6}$$

$$-i\omega f_l + \frac{l}{2l-1} ikv f_{l-1} + \frac{l+1}{2l+3} ikv f_{l+1} \;=\; -\nu_l f_l, (l > 3), \tag{7}$$

where $\nu_l = \left(l\left(l+1\right)/2\right)\nu_1$, $\nu_1 = 4\pi N_e Z e^4 \ell n\left(\Lambda\right)/(m_e^2 v^3)$, $\lambda_t = v/\nu_1$, and

$$S_0^{lin} \;=\; \frac{ikv}{3} u \frac{\partial F_0}{\partial v}, \tag{8}$$

$$S_1^{lin} \;=\; \tilde{E}\frac{\partial F_0}{\partial v} - i\omega u \frac{\partial F_0}{\partial v}, \tag{9}$$

$$S_2^{lin} \;=\; \frac{2ikv}{3}u\frac{\partial F_0}{\partial v}, \tag{10}$$

where $\tilde{E} = eE/m_e$. Electron-electron collisions are retained only for $l = 0$ because electron-ion collisions do not contribute to the $l = 0$ equation and, for $l > 0$, the electron-ion collision rate is much faster than the electron-electron rate if $Z \gg 1$. The coupling of the acoustic waves to the light waves is from the terms, S_l^{nl}, given by

$$S_0^{nl} \;=\; \frac{1}{6}\left[\nu_1|v_E|^2\left(\delta(v) + v\frac{\partial}{\partial v}\frac{1}{v}\right) + \frac{\partial|v_E|^2}{\partial t}\left(\frac{3}{2v} + \frac{v}{2}\frac{\partial}{\partial v}\frac{1}{v}\right)\right]\frac{\partial F_0}{\partial v}, \tag{11}$$

$$S_1^{nl} \;=\; \frac{ik}{2}|v_E|^2\left[1 + \left(2\cos^2\phi_0 + 1\right)\frac{v^2}{10}\frac{\partial}{\partial v}\frac{1}{v}\right]\frac{\partial F_0}{\partial v}, \tag{12}$$

$$S_2^{nl} \;=\; \frac{1}{6}\left(\nu_1|v_E|^2 v^4\frac{\partial}{\partial v}\frac{1}{v^4} + \frac{\partial|v_E|^2}{\partial t}\frac{v}{2}\frac{\partial}{\partial v}\frac{1}{v}\right)\frac{\partial F_0}{\partial v}\left(3\cos^2\phi_0 - 1\right), \tag{13}$$

$$S_3^{nl} \;=\; \frac{ik}{20}|v_E|^2\left(3\cos^2\phi_0 - 1\right)v^2\frac{\partial}{\partial v}\frac{1}{v}\frac{\partial F_0}{\partial v}, \tag{14}$$

where $\cos^2\phi_0 = |k\cdot E_0|^2/k^2E_0^2$. Because we are interested in the transition from collisional to collisionless behavior, the neglect of electron-electron collisions is justified for frequencies, $|\omega| \sim \nu_1 > \nu_{ee}$ if $Z > 1$.[16] In the collisional limit defined by $k\lambda_{th} = k\lambda_t(v_e) \ll 1$, S_0^{nl} is the dominant nonlinear term and only f_0 and f_1 need be kept.

In Appendix A, by generalizing Eqs. (A3) and (A4) of Reference [15] given by Eqs. (A7) and (A9), we obtain expressions for f_0 and f_1 in terms of F_0, E, *etc.* namely,

$$\Omega^2 f_0 \;=\; \frac{ikv}{3}\frac{\partial F_0}{\partial v}\left(-\tilde{E} + \nu_1 u\right) + \left(\tilde{\nu_1}S_0^{nl} - \frac{ikv}{3}\tilde{S}_1^{nl}\right), \tag{15}$$

$$\Omega^2 f_1 \;=\; \frac{\partial F_0}{\partial v}\left(u\left(\Omega^2 + i\omega\nu_1\right) - i\omega\tilde{E}\right) - \left(ikvS_0^{nl} + i\omega\tilde{S}_1^{nl}\right), \tag{16}$$

where

$$\nu_{l,\omega} = \nu_l - i\omega, \tag{17}$$

$$\tilde{\nu}_{l,\omega} = \nu_{l,\omega} + \frac{(l+1)^2}{(2l+1)(2l+3)}\frac{k^2v^2}{\tilde{\nu}_{l+1,\omega}}, \tag{18}$$

and, for convenience, we introduce

$$\Omega^2 = -i\omega\tilde{\nu_1} + \frac{k^2v^2}{3}, \tag{19}$$

$$H_1 = \tilde{\nu}_{1,\omega}/\nu_{1,\omega}. \tag{20}$$

The low frequency beat pressure perturbation, $m_eN_cv_E^2$ is related to the high frequency light waves, $E_0(k_0,\omega_0)$ and $E(k\pm k_0,\omega\pm\omega_0)$ by

$$|v_E|^2 = \left(E_0 E^* \left(k + k_0, \omega + \omega_0\right) + E_0^* E \left(k - k_0, \omega - \omega_0\right)\right) / 4\pi m_e N_c, \tag{21}$$

where N_c is the plasma critical density ($\omega_0^2 = 4\pi N_c e^2/m_e$).

The plasma response is completed with the cold ion fluid equations for a single species,

$$-i\omega n_i + ikN_i u_i = 0 \tag{22}$$

$$-i\omega N_i m_i u_i = ZN_i m_e \tilde{E} + R_{ie} \tag{23}$$

where the ion-electron momentum exchange rate is

$$R_{ie} = \frac{4\pi m_e}{3} \int_0^\infty dv v^3 \nu_1 f_1 \tag{24}$$

and, with the quasi-neutrality approximation, the perturbed electron and ion charge densities are,

$$n_e = 4\pi \int_0^\infty dv v^2 f_0 = Z n_i \tag{25}$$

The set of equations is completed with the wave equations for the scattered light waves,

$$D_\pm E^\pm = D\left(k \pm k_0, \omega \pm \omega_0\right) E\left(k \pm k_0, \omega \pm \omega_0\right) = \frac{4\pi e^2}{m_e} E_0 n_e\left(k, \omega\right), \tag{26}$$

where

$$D_\pm = \left(\omega \pm \omega_0\right)^2 - 2i\nu_{abs}\left(\omega \pm \omega_0\right) - \omega_{pe}^2 - c^2\left(k \pm k_0\right)^2. \tag{27}$$

The inverse bremsstrahlung absorption rate is, $\nu_{abs} = \left(N_e/2N_c\right)\nu_{ei}$ where $\nu_{ei} = 4\sqrt{(2\pi)} N_e Z e^4 \ln\Lambda / \left(3 m_e^2 v_e^3\right) = \nu_1^{th}/(3\sqrt{\pi/2})$, $v_e = \sqrt{T_e/m_e}$, and $\nu_1^{th} = \nu_1\left(v_e\right)$. The collision frequency ν_1^{th} and the mean free path $\lambda_{th} = v_e/\nu_1^{th}$, are related to the Braginskii electron-ion collision frequency and mean free path[17] by $\nu_1^{th} = 3\sqrt{(\pi/2)}\nu_{ei}$ and $\lambda_{th} = \lambda_{ei}/(3\sqrt{(\pi/2)})$.

The generalized dispersion relation for scattering light waves from thermally and ponderomotively driven acoustic waves is given by,

$$\varepsilon\left(k, \omega\right) = \frac{-1}{4} k^2 v_0^2 \chi_e\left(k, \omega\right) \left(\frac{1}{D\left(k + k_0, \omega + \omega_0\right)} + \frac{1}{D\left(k - k_0, \omega - \omega_0\right)}\right) \tag{28}$$

where

$$\varepsilon\left(k, \omega\right) = \frac{\omega^2}{k^2 C_s^2} + \eta\left(\sqrt{2/\pi}/3 + \eta_e J_1\right) - \frac{\left(1 + \eta_e J_4\right)\left(1 + \eta J_4\right)}{J_7}, \tag{29}$$

where $\eta = \eta_e = i\omega/kv_e/k\lambda_{th}$, and

$$\chi_e(k,\omega) = -2\frac{\omega_{pe}^2}{k^2 v_e^2}\left(\frac{(1+\eta_e J_4)}{J_7}\bar{n}_e - \eta_e \bar{R}_{ie}\right) \tag{30}$$

where $\bar{n}_e = \bar{n}_{e,s} + \bar{n}_{e,a}$.

$$\bar{n}_{e,s} = -J_7 + \frac{1}{6}J_9 + \frac{1}{3\eta_e k^2\lambda_{th}^2}\left(J_6 - i\frac{\omega_E}{2\nu_1^{th}}(J_9 - 3J_7)\right) \tag{31}$$

$$\begin{aligned}
\bar{n}_{e,a} &= \bar{n}_{e,a,1} + \bar{n}_{e,a,2} + \bar{n}_{e,a,3} && (32)\\
\bar{n}_{e,a,1} &= -\frac{\psi_0\eta}{2}\left(3J_2 - \frac{1}{2}J_4 + i\frac{\omega-\omega_E}{2\nu_1^{th}}J_6\right) && (33)\\
\bar{n}_{e,a,2} &= \frac{\psi_0}{6}\frac{\nu_1^{th}}{(-i\omega)}\left(3J_4 - 3\Gamma(-1) - \frac{1}{2}\left(J_6 - \sqrt{2/\pi}\right)\right.\\
&\quad + \left. i\left(\frac{\omega-\omega_E}{\nu_1^{th}}\right)(J_8 - 3)\right) && (34)\\
\bar{n}_{e,a,3} &= \frac{\psi_0}{2k^2\lambda_{th}^2}\left(3J_{-1} - \frac{1}{2}J_1 + i\frac{\omega-\omega_E}{2\nu_1^{th}}J_3\right) && (35)
\end{aligned}$$

where $\psi_0 = 3\cos^2\phi_0 - 1$, $-i\omega_E = \partial \ln(|v_E|)^2/\partial t$, and $\Gamma(n) = \sqrt{2/\pi}\int_0^\infty dx x^n \exp(-x^2/2)$. The divergent terms, $\Gamma(-1)$ and J_{-1}, combine to produce a finite result as shown in Appendix B. The contributions from the friction force are:

$$\begin{aligned}
\bar{R}_{ie} &= \bar{R}_{ie,1} + \bar{R}_{ie,2} && (36)\\
\bar{R}_{ie,1} &= -J_4 + \frac{1}{6}J_6 + \frac{1}{3\eta_e k^2\lambda_{th}^2}\left(J_3 - i\frac{\omega_E}{2\nu_1^{th}}(J_6 - 3J_4)\right) && (37)\\
\bar{R}_{ie,2} &= \frac{\psi_0}{2}\left(\eta\left(3K_{-1} - \frac{1}{2}K_1\right) - \frac{\omega(\omega-\omega_E)}{2k^2 v_e^2}K_4\right.\\
&\quad - \frac{1}{k^2\lambda_{th}^2}\left(3K_{-4} - \frac{1}{2}K_{-2}\right) - \eta\left(1 - \frac{\omega_E}{\omega}K_1\right)\Bigg) && (38)
\end{aligned}$$

In the notation introduced by Epperlein[13],

$$J_m = \sqrt{\frac{2}{\pi}}\int_0^\infty dV \frac{V^m \exp(-V^2/2)}{V^5 - 3\eta_e(1 - i\omega/\nu_1)H_1} \tag{39}$$

where H_1 is defined by Eq. (20). The additional integral needed is

$$K_m = \sqrt{\frac{2}{\pi}}\int_0^\infty dV \frac{V^m \exp(-V^2/2)(H_1 - 1)}{V^5 - 3\eta_e(1 - i\omega/\nu_1)H_1} \tag{40}$$

Given the negative powers of V in the integrand of K_m in Eq. (38), we note that, because $H_1 - 1 \to 0$ as $V \to 0$, the integrals are well behaved provided $|\omega|$ is not zero. A distinction

between η and η_e has been maintained to facilitate a subsequent discussion of the influence of electron self-collisions.

Setting the LHS of Eq.(28) to zero recovers the linear ion acoustic dispersion equation obtained by Epperlein[13] which showed (see Fig. 1 of reference[13]) that the electron damping rate of ion acoustic waves, ν_a, was given by the collisionless Landau value when $k\lambda_{th} \geq 200$ and ν_a/kC_s, the ratio of the damping to the isothermal acoustic frequency where $C_s = \sqrt{(ZT_e/m_i)}$, reached a maximum when $k\lambda_{th} \sim .01$. The ion acoustic wave frequency, not shown in reference[13], is $\sqrt{\frac{5}{3}}kC_s$ for $k\lambda_{th} << 1$ and kC_s for $k\lambda_{th} >> 1$. These results are also shown in Fig. 1 of this manuscript. In the collisionless limit, the RHS of Eq.(28) reduces to the familiar result for ponderomotively driven stimulated Brillouin scattering and filamentation if $|\eta| << 1$ in which case $J_7 \sim 1$, $J_9 \sim 3$, $\eta J_4 << 1$, and the real part of the term in brackets in Eq. (30) equals $-1/2$. For reference, the dispersion relation in the collisionless Vlasov theory has a form similar to Eq. (28), namely,

$$\varepsilon(k,\omega) = \frac{k^2 v_0^2}{4}\chi_e\left(k,\omega\right)\left(1+\chi_i\left(k,\omega\right)\right)\left(\frac{1}{D\left(k+k_0,\omega+\omega_0\right)}+\frac{1}{D\left(k-k_0,\omega-\omega_0\right)}\right) \qquad (41)$$

In the quasi-neutral limit, the collisionless dielectric function is given by $\epsilon = \chi_e + \chi_i$, $|\chi_e| \gg 1$, and $\chi_e = (1 + \xi_e Z(\xi_e))/k^2\lambda_{de}^2$ where the plasma dispersion function, $Z(\xi) = \sqrt{1/\pi}\int_{-\infty}^{\infty} dx \exp(-x^2)/(x-\xi)$ and $\xi_e = \omega/(\sqrt{2}kv_e)$. In the cold ion limit $\chi_i = -\omega_{pi}^2/\omega^2$. Because the phase velocity is much less than the electron thermal velocity, $Z(\xi_e)) \sim i\sqrt{\pi}$, and to lowest order, $\omega = kC_s(1 - i\sqrt{\pi Z m_e/2m_i}/2) = kC_s(1 - .01i\sqrt{2Z/A})$. Here, A is the atomic mass.

In Ref. [20], the wavelength dependence of the ion acoustic damping rate was computed with electron-electron collisions included. In Fig. 1, this Z dependence of the damping rate is compared to that without electron-electron collisions. Over the range of interest to the SBS growth rates shown in Fig. 2, the damping rate without self-collisions is nearly the same as that for the charge state $Z = 64$, with electron self-collisions included. The damping rate for $Z = 8$ with electron self-collisions is lower as shown. Thus, caution should be taken before applying to low Z plasmas the growth rates that are obtained in the subsequent sections which neglect self-collisions.

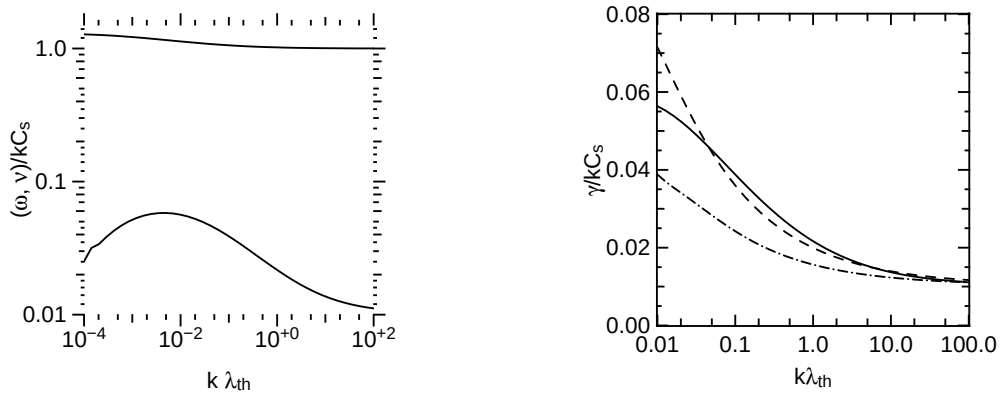

FIG. 1: (*left*) The frequency and cold-ion damping rate of acoustic waves is displayed as a function of $k\lambda_{th}$. (*right*) The ion acoustic damping rate in units of kC_s is shown versus $k\lambda_{th}$ as given by the solution to Eq. (29) (solid) and as given in Reference [20] for $Z = 64$ (dash) and $Z = 8$ (dashdot).

III. CONVECTIVE TEMPORAL GROWTH RATE FOR STIMULATED BRILLOUIN BACKSCATTER

Consider the important case of three-wave Brillouin backscatter where $k = 2k_0 + \delta k$, $|\delta k| << k_0$, and $E\left(k + k_0, \omega + \omega_0\right)$ is not resonant. Using the fact that the incident light wave satisfies $\omega_0^2 = \omega_{pe}^2 + c^2 k_0^2$,

$$D\left(k - k_0, \omega - \omega_0\right) = D_- = 2\omega_0(-\omega - v_{g0}\delta k + i\nu_{abs}) \tag{42}$$

where $v_{g0} = c^2 k_0/\omega_0$ is the incident light wave group velocity. With this approximation, Eq.(28) becomes,

$$\omega - \omega_a - d\Omega + i\nu_{abs} + \frac{1}{8}k^2 v_0^2 \chi_e\left(k, \omega\right)/\omega_0 \varepsilon\left(k, \omega\right) = 0, \tag{43}$$

where $d\Omega = v_{g0}\delta k - \omega_a$ with $\omega_a \equiv kC_s$. In the collisionless limit and $ZT_e/T_i >> 1$ so that ion Landau damping is much smaller than the small electron Landau damping, ν_a,

$\varepsilon(k,\omega) \approx (\omega - \omega_a - i\nu_a)\partial\varepsilon/\partial\omega$ where $\partial\varepsilon/\partial\omega \approx 2\omega/(kC_s)^2$. This quadratic equation gives the weak coupling ($|\Im(\omega)| \ll |\omega| \sim \omega_a$) convective SBS growth rate,

$$\omega = \omega_a + \frac{1}{2}d\Omega - \frac{i}{2}(\nu_a + \nu_{abs}) \pm \left[\frac{1}{4}\left(d\Omega - i\left(\nu_a - \nu_{abs}\right)\right)^2 - \gamma_{0,sbs}^2\right]^{1/2}, \tag{44}$$

where

$$\gamma_{0,sbs}^2 = \frac{1}{16}\frac{N_e v_0^2 \omega_a \omega_0}{N_c v_e^2}. \tag{45}$$

The maximum growth rate occurs for perfect frequency matching, $d\Omega = 0$ for which $\delta k = -2C_s\omega_0/c^2$. For arbitrary $k\lambda_{th}$, we solve Eq.(43) for $\hat{\omega} = \omega/\omega_a$ given the ratio of the electron density to the critical density, N_e/N_c, and the coupling strength, $\beta_c = \omega_0 v_0^2/4\omega_a v_e^2$ so that $\gamma_{0,sbs}^2/\omega_a^2 = (N_e/4N_c)\beta_c$. The light absorption rate is then $\hat{\nu}_{abs} \equiv \nu_{abs}/\omega_a = 1/(3\sqrt{2\pi})(N_e/N_c)\sqrt{(m_i/(Zm_e)}\,(k\lambda_{th})^{-1}$. Clearly, the light absorption rate becomes comparable to the acoustic frequency in the long wavelength limit.

In Fig. 2, the growth rate of SBS is shown as a function of $k\lambda_{th}$ for $N_e/N_c = .05$ and $\beta_c = 0.2$ with thermal and ponderomotive coupling and with only ponderomotive coupling. The cutoff at long wavelengths is due to inverse bremsstrahlung absorption of the scattered light wave. At short wavelengths, $k\lambda_{th} \gtrsim 60$, only ponderomotive coupling is important. Without light or acoustic wave absorption all cases have the same growth rate which in the collisionless limit is $.05\omega_a$. These calculations show a strong enhancement of the backward SBS growth rate above the collisionless rate for $k\lambda_{th} < 10$ provided that the electron density is low enough that collisional absorption of the light wave is weak.

Previous treatments of thermal enhancement of backward SBS have relied on fluid equations with Braginskii transport[18] and with nonlocal transport [8],[9],[19]. Taking advantage of the fact the dominant terms in the electron temperature equation are the inverse bremsstrahlung heating and the heat flow, the fluid dispersion equation for these latter cases is given by,

$$(\omega - \omega_a - d\Omega + i\nu_{abs})(\omega^2 + 2i\omega\nu_a - \omega_a^2) + \frac{1}{8}\frac{v_0^2}{v_e^2}\frac{N_e}{N_c}\omega_0\omega_a^2 A_k = 0, \tag{46}$$

where A_k encompasses the thermal enhancement of the coupling of the acoustic wave to the light waves. For A_k given by,

$$A_k = 1 + \frac{3\pi}{64}\frac{(1 + rq_k)}{(k\lambda_{ei})^2}, \tag{47}$$

the results of Short and Epperlein[8] are obtained if

$$rq_k = (21k\lambda_e)^{1.44}, \tag{48}$$

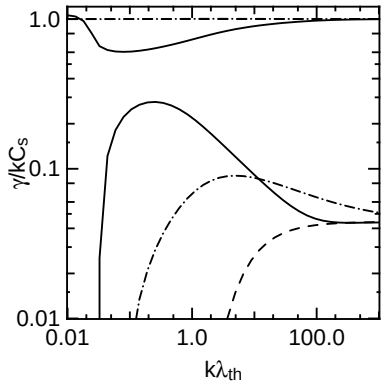

FIG. 2: The real (upper set of curves) and imaginary parts (lower set) of $\omega/(kC_s)$ are displayed as a function of $k\lambda_{th}$. The solid curves with $\psi_0 = -1$ that is, $k\perp E$, are the kinetic frequency and growth rates ; the dashed curves are the solution to the collisionless dispersion equation (41); the dash-dot curves are for the Bychenkov model [19] with $Z = 64$.The fluid models of Ref. [8] and that of [19] agree for $Z = 64$.

and the results of Rose and DuBois [9] if $rq_k = 50k\lambda_e$. Here, $\lambda_e = \sqrt{Z}\lambda_{th} = \sqrt{Z}\lambda_{ei}/3.76$ in the Lorentz gas (high Z) limit. A more recent treatment by Bychenkov *et al.* [19] uses,

$$A_k = 1 + 2\left(\frac{0.074}{(k\lambda_{ei})^2} + \frac{0.88Z^{5/7}}{(k\lambda_{ei})^{4/7}} + \frac{2.54Z}{(1+5.5Z(k\lambda_{ei})^2}\right). \tag{49}$$

The equations derived in our paper by introducing a complex frequency ω to all orders in the equations for the Legendre polynomial coefficients (apart from the neglect of electron-electron collisions) extend this last treatment which is also based on the results derived in Reference[15].

In Fig. (2), the growth rates obtained by solving Eq. (46) with A_k given by Eq. (49) is also shown. This model does not converge to the ponderomotive growth rate as quickly as our Lorentz model because it neglects the acoustic wave frequency compared with the electron-

ion collision frequency in the higher order Legendre polynominal coefficients. The merging of the ponderomotive growth rate with the kinetic solution occurs when $Re(\omega) \simeq \nu_{ei}$, *viz.*, for $k\lambda_{th} \simeq 60$ in Fig. (2). There are substantial differences at longer wavelengths where $Re(\omega) \ll \nu_{ei}$. One source of the difference is the influence of electron self-collisions which are neglected in Eq. (43) and treated with a linearized Landau operator in Ref. [19]. As shown in Fig. 1, self-collisions had little influence on the linear properties of ion acoustic waves for high Z plasma over the range of $k\lambda_{th}$ shown in Fig. 2.

IV. CONVECTIVE TEMPORAL GROWTH RATE FOR STIMULATED BRILLOUIN FORWARD SCATTER

Small angle scattering of light involves long wavelengths such that $k << k_0$ and $k\lambda_{ei} \lesssim 1$ even if $k_0\lambda_{ei} \gg 1$. Thus, thermal enhancement of the scattering rate is not necessarily accompanied by a strong damping of the scattered light wave. Despite the much lower frequency of the ion acoustic wave, the upper light sideband, $E\left(k+k_0, \omega+\omega_0\right)$ can still be neglected because $k \gg k_0 C_s/c$ except for very small angles. The weakly coupled SBS growth rate given in Eq. (44) for perfect matching and with damping neglected is,

$$\gamma_0 \;=\; \sqrt{\omega_a \omega_0 \alpha_e/8} \tag{50}$$

$$\alpha_e \;=\; (1/2)(N_e/N_c)(v_0^2/v_e^2) \tag{51}$$

where α_e is a measure of the strength of the parametric coupling. Because of the large ratio of ω_0 to ω_a, $[\omega_0/(kC_s) \sim 10^3$ when $k = k_0]$, forward SBS is easily driven strongly with $|\omega| \gtrsim \omega_a$. In Fig. 3, the growth rate is shown as a function of the ion acoustic wavenumber times the electron-ion mean free path for a fixed value of $k_0\lambda_{th} = 100$ for which the light wave damping is relatively weak. The upper set of relatively flat curves in this figure are the frequencies for which the growth rate is maximum. The lower dashed curve and the solid curve that merges with it at large $k\lambda_{th}$ are the growth rates for forward SBS. Since, in this case, the ponderomotive growth rate (dashed line) satisfies the weakly driven approximation for all $k\lambda_{th}$, the frequency for which the growth rate is a maximum is the cold-ion, isothermal acoustic frequency, $kC_s = k\sqrt{ZT_e/m_i}$ to which all (complex) frequencies are normalized. The total growth rate is much larger than the ponderomotive one at long wavelengths and is a strongly driven one. The frequency that maximizes this growth rate differs from the

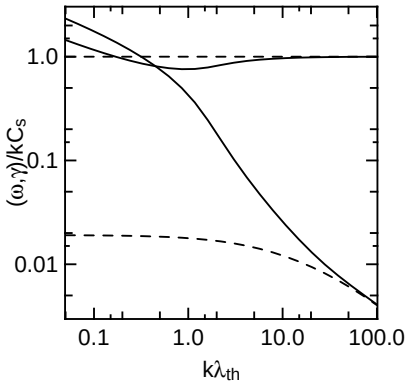

FIG. 3: The frequency and growth rate of stimulated Brillouin forward scatter is displayed as a function of $k\lambda_{th}$ for the solution to the collisionless dispersion Eq. (41) (dashed) and for ponderomotive and thermal dispersion Eq.(28). The coupling parameter, $\alpha_e = 10^{-6}$, $Z/A = 1/2$, $\psi = -1$.

frequency shown in Fig. 1 as one expects for strongly driven SBS[2, 21]. For short wavelength ion acoustic waves, there is no thermal enhancement above the ponderomotive rate once the frequency of the ion wave exceeds the electron-ion collision frequency, ν_{ei}. Taking $\omega = kC_s$, we find the thermal contributions are small when $k\lambda_t > \sqrt{(m_i/Zm_e)}$.

V. CONVECTIVE TEMPORAL GROWTH RATE FOR FILAMENTATION

The dispersion relation (28) also describes a purely growing 4-wave instability for which $D(k - k_0, \omega - \omega_0)$ and $D(k + k_0, \omega + \omega_0)$ contribute equally and $k \perp k_0$. Using the dispersion relation for the pump, $\omega_0^2 = \omega_{pe}^2 + c^2k_0^2$, the scattered light dispersion can be simplified as $D(k \pm k_0, \omega \pm \omega_0) = \pm 2i\gamma\omega_0 - c^2k^2 \pm i\nu_{abs}\omega_0$ where $\omega = i\gamma$. The ponderomotively driven growth rate is determined from the equation,

$$\left(\gamma\left(\gamma+\nu_a\right)+\omega_a^2\right)\left(\left(\gamma+\nu_{abs}\right)^2+\frac{c^4k^4}{4\omega_0^2}\right)=\frac{k^2v_0^2}{4\omega_0^2}\frac{c^2k^2}{2}\omega_{pi}^2 \tag{52}$$

If the growth rate satisfies the inequality,

$$\gamma>\omega_a,\nu_{abs}, \tag{53}$$

then the maximum growth rate is

$$\gamma_p^{max}=\frac{1}{8}\frac{v_0^2}{v_e^2}\frac{\omega_{pe}^2}{\omega_0^2}\omega_0 \tag{54}$$

for

$$k_p=\frac{1}{2}\frac{v_0}{v_e}\frac{\omega_{pe}}{\omega_0}\frac{\omega_0}{c} \tag{55}$$

At large wavenumbers, $k>\sqrt{2}k_p$, diffraction overcomes the focusing effects and filamentation is stable.

Consider the relative strength of filamentation and forward SBS driven ponderomotively. Because damping by the ions is assumed negligible, $\omega_a/(2\nu_a)\sim 50>>1$, $\gamma>\nu_a$, and the weakly damped SBS growth rate given by Eq. (50) applies. Considering the ponderomotive growth rate for weakly-damped forward SBS and filamentation at the wavenumber, k_p, divided by the acoustic frequency, k_pC_s,

$$\frac{\gamma_{sbs}^{wd}(k_p)}{\omega_a(k_p)} = \frac{\sqrt{2}}{4}\sqrt{\frac{\omega_{pe}}{\omega_0}\frac{v_0}{v_e}\frac{c}{C_s}} \tag{56}$$

$$\frac{\gamma_{fil}(k_p)}{\omega_a(k_p)} = \frac{1}{4}\frac{\omega_{pe}}{\omega_0}\frac{v_0}{v_e}\frac{c}{C_s}, \tag{57}$$

one notes the single parameter, $\rho_p=(\omega_{pe}/\omega_0)(v_0/v_e)(c/C_s)$, determines which growth rate is faster at that wavenumber. For the parameters of the example given in Fig. 3, $\rho_p\sim 1.4$ for which the two rates are comparable. Moreover, the filamentation instability barely satisfies the supersonic criterion (Eq. (53)) made in obtaining Eq. (54) and is limited to long wavelengths, $\lambda_p/\lambda_0=k_0/k_p=1.4\times10^3$ for which kinetic effects on the thermal contributions are minimal. Thus, we will consider an example of the filamentation response when $\alpha_e=1\times10^{-4}$, one hundred times the value in Fig. 3

Thermal enhancement of the ponderomotive growth both increases the maximum growth rate and extends the range of unstable wavenumbers. As with SBS, thermally enhanced growth rates have been found previously by multiplying the right hand side of Eq. (52) by the factor A_k as in Eq. 46. In Fig. 4, the ponderomotive growth rate, the growth rate

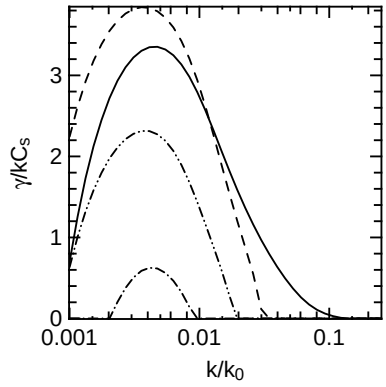

FIG. 4: The filamentation growth rate, normalized to the isothermal acoustic frequency, $k\sqrt{ZT_e/m_i}$, is plotted vs the wavenumber divided by the laser wavenumber, ω_0/c from Eq. (28) (solid), for the collisionless dispersion Eq.(41) (dash-dot), for the thermally enhanced rate with A_k given by Eq. (49)and $Z = 64$ (dash) , and for rate thermally enhanced by A_k and $Z = 8$(dash-dot-dot). The parameters are $T_e = 2$ keV, $N_e/N_c = .05$, $v_0/v_e = 0.063$, and $k_0\lambda_{ei} = 3.76$ $k_0\lambda_{th} = 376$. In all cases, $Z/A = 1/2$ and $\psi_0 = -1$.

enhanced by the thermal factor, A_k, and the growth rate from Eq. (28) are plotted for $T_e = 2$ keV, $Z = 64$, $Z/A = 1/2$, $N_e/N_c = .05$, $v_0/v_e = 0.063$, and $k_0\lambda_{ei} = 3.76 k_0\lambda_{th} = 376$. For the ponderomotive rate, Z is not a factor . Although the maximum growth rates are larger than ω_a, the growth rate is still larger than the ponderomotive rate unlike the SBS growth which relaxes to the ponderomotive rate once $\Re\omega \sim \omega_a$ and $k_0\lambda_{ei} >> 1$. Also, our Lorentz gas results have the peculiar behavior that the growth rate has a "tail" above the diffraction cutoff for the other curves. This behavior has its source in terms like the third term in Eq. (31) which diverges for finite k as $\gamma \to 0$. This behavior does not occur if electron-electron collisions are kept[20] because, then, the left hand side of Eq. (15) remains nonzero as $\gamma \to 0$ and $v \to 0$ so that the integrands of the integrals (Eqs. (39) and (40))

that define J_m and K_m respectively remain well behaved for all k, ω.

VI. CONCLUSIONS

We have studied stimulated Brillouin scattering and filamentation for arbitrary electron-ion spatial and temporal collisionality, that is, for any value of $k\lambda_{ei}$ and ω/ν_{ei}. Of particular interest is the transition from thermally driven SBS to ponderomotively driven SBS. We find that once $\omega > \nu_{ei}$ and $k\lambda_{ei} > 1$, the thermal forces are insignificant compared with the ponderomotive forces. Because we neglected electron self-collisions altogether , the results are strictly valid only for high-Z plasma. One approach to including self-collisions might be to use a Krook operator in Eq. (3) for C_{ee}. The simplest form is the nonconservative $-\nu_{ee}(v_e)f_0$ which has the effect that $\eta_e = (i\omega - \nu_{ee})/kv_e/k\lambda_{th}$ but η remains unchanged. That change has the desirable effect that the integrals defining J_m and K_m are well behaved as $|\omega| \to 0$ and $v \to 0$. However, with this approximation for self-collisions, the linear dispersion properties of the ion acoustic waves in the long wavelength limit differ markedly from the known properties of the ion acoustic waves with self-collisions. Even use of a form that conserves density was inadequate in that self-collisions either had no effect or too strong an effect on the linear dispersion. However, electron self-collisions are known to be important for $k\lambda_{ei} \sim 1 - 10$ where only a few Legendre polynomials are needed to represent the dominant electron-ion collisions. More importantly, this neglect doesn't affect the general conclusion about the transition from thermal to ponderomotive stimulated scatter.

The filamentation instability is a purely growing instability. Here there is no "transition" to purely ponderomotively driven scatter even when the growth rate exceeds the ion acoustic normal mode frequency for the wavelength of the unstable mode. Thus, for the same wavelength, a thermally driven filament and a ponderomotively driven traveling acoustic wave may co-exist for the same linear dispersion relation. This behavior presents fluid codes[22] that use model equations to represent intricate light wave propagation in hot, dense plasma clear difficulties if SBS and filamentation are to be treated faithfully.

RLB is grateful to the Princeton Plasma Physics Laboratory, in particular Drs. William Tang and Nathaniel Fisch, where this work was done for their hospitality. The work of RLB was performed under the auspices of the U.S. Department of Energy by the University of California, Lawrence Livermore National Laboratory under contract No. W-7405-Eng-48.

APPENDIX A: THE REDUCTION OF HIGHER ORDER LEGENDRE TERMS BY USE OF CONTINUED FRACTIONS

We start with Eqns. (3)-(14). For $l > 3$, the higher Legendre polynomials can be found in terms of the lower ones,

$$\tilde{\nu_l} f_l = -ikv \left(\frac{l}{(2l-1)} \right) f_{l-1} \tag{A1}$$

where $\tilde{\nu_l}$ is defined by Eq. (18). Substituting in turn for f_{l+1} in the equation for f_l for $l = 3, 2$, we obtain the equation for f_1,

$$\tilde{\nu_1} f_1 + ikv f_0 = -\frac{2}{5} \frac{ikv}{\tilde{\nu_2}} \left(S_2 - \frac{3}{7} \frac{ikv}{\tilde{\nu_3}} S_3 \right) + S_1. \tag{A2}$$

The terms ${\tilde{\nu_1}}^{-1}$ for $l = 2, 3$ are eliminated by using Eq. (18) to arrive at

$$\tilde{\nu_1} f_1 + ikv f_0 = S_1^{lin} + (\nu_1 - i\omega)(H_1 - 1) u \frac{\partial F_0}{\partial v} + \tilde{S}_1^{nl} \tag{A3}$$

$$\tilde{S}_1^{nl} = \tilde{S}_{1,s}^{nl} + \tilde{S}_{1,a}^{nl} \tag{A4}$$

where

$$\tilde{S}_{1,s}^{nl} = ik \frac{|v_E|^2}{2} \left(\frac{\partial F_0}{\partial v} + \frac{v^2}{6} \frac{\partial}{\partial v} \left(\frac{1}{v} \frac{\partial F_0}{\partial v} \right) \right) \tag{A5}$$

$$\tilde{S}_{1,a}^{nl} = -i\psi_0 \left(\frac{|v_E|^2}{6} \right) \frac{3}{2kv} (\nu_1 - i\omega)(H_1 - 1) \left[\nu_1 v^4 \frac{\partial}{\partial v} \left(\frac{1}{v^4} \frac{\partial F_0}{\partial v} \right) + \frac{1}{2} \left(i\omega - \nu_2 + \frac{\partial}{\partial t} ln|v_E|^2 \right) v \frac{\partial}{\partial v} \left(\frac{1}{v} \frac{\partial F_0}{\partial v} \right) \right] \tag{A6}$$

where $\psi_0 = 3\cos^2\phi_0 - 1$ and H_1 is defined in Eq. (20). Substituting f_0 into Eq. (A3), we obtain the equation,

$$\Omega^2 f_1 = \frac{\partial F_0}{\partial v} \left(u \left(\Omega^2 + i\omega\nu_1 \right) - i\omega\tilde{E} \right) + \left(-ikv S_0^{nl} - i\omega \tilde{S}_1^{nl} \right) \tag{A7}$$

where

$$\Omega^2 = -i\omega\tilde{\nu_1} + \frac{k^2 v^2}{3}. \tag{A8}$$

Substituting Eq. (A3) for f_1 into Eq. (3) for f_0, we obtain the equation,

$$\Omega^2 f_0 = \frac{ikv}{3} \frac{\partial F_0}{\partial v} \left(-\tilde{E} + \nu_1 u \right) + \left(\tilde{\nu_1} S_0^{nl} - \frac{ikv}{3} \tilde{S}_1^{nl} \right) \tag{A9}$$

APPENDIX B: THE NONDIVERGENCE OF CERTAIN TERMS

Here, we demonstrate that the divergent terms proportional to $\Gamma(-1)$ in Eq. (34) and J_{-1} in Eq. (35) combine to produce a finite result. Using the definition of η_e the integrand of the sum of these terms is proportional to,

$$I = \frac{\nu_1^{th}}{-i\omega V}\left(1 + \frac{3\eta_e}{V^5 - 3\eta_e(1 - i\omega/\nu_1)H_1}\right) \tag{B1}$$

$$= \frac{\nu_1^{th}}{-i\omega V}\left(\frac{V^5 + i\omega H_1/\nu_1 - 3\eta_e(H_1 - 1)}{V^5 - 3\eta_e\,(1 - i\omega/\nu_1)\,H_1}\right) \tag{B2}$$

Since $H_1 - 1 \to 0$ faster than V and $\nu_1^{-1} \sim V^3$, this integral is well behaved if $|\omega|$ is nonzero.

[1] J. F. Drake, P. K. Kaw, Y. C. Lee, *et al*, Phys. Fluids **17**, 778 (1974)

[2] B. I. Cohen and C. E. Max, Phys. Fluids **22**, 1115 (1979)

[3] L. Spitzer and R. Härm, Phys. Rev. **89**, 977 (1953)

[4] W. L. Kruer, *The Physics of Laser Plasma Interactions* (Addison-Wesley, New York, 1988)

[5] J. R. Albritton, Phys. Rev. Lett. **50**, 2078 (1983); J. R. Albritton,E. A. Williams, I. B. Bernstein, and K. P. Swartz, Phys. Rev. Lett. **57**, 1887 (1986)

[6] J. F. Luciani, P. Mora, and J. Virmont, Phys. Rev. Lett. **51**, 1664 (1983)

[7] E. M. Epperlein, Phys. Rev. Lett. **65**, 2145 (1990)

[8] R. W. Short and E. M. Epperlein, Phys. Rev. Lett. **68**, 3307 (1992).

[9] H. A. Rose and D. F. DuBois, Phys. Fluids B**4**, 1394 (1992).

[10] G. W. Hammet and F. W. Perkins, Phys. Rev. Lett. **64**, 3019 (1990)

[11] T. B. Kaiser, B. I. Cohen, R. L. Berger, *et al*, Phys. Plasmas **1**, 1287 (1994)

[12] A. R. Bell, Phys. Fluids **26**, 279 (1983)

[13] E. M. Epperlein, R. W. Short, and A. Simon, Phys. Rev. Lett. **69**,1765 (1992).

[14] E. M. Epperlein, Phys. Plasmas **1**, 109 (1994).

[15] A. V. Brantov, V. Yu. Bychenkov, V. T. Tikhonchuk, and W. Rozmus, Phys. Plasmas **5**, 2742 (1998).

[16] The exception to this validity condition occurs for filamentation near threshold where $|\omega| \to 0$ and some moments of the distribution functions, f_l, are divergent unless electron-electron collisions are retained.

[17] S. I. Braginskii, in *Reviews of Plasma Physics*, edited by M. A. Leontovich (Consulting Bureau, New York, 1965), Vol. 1, p. 215

[18] B. L. Cragin and J. A. Fejer, Radio Sci. **9**, 1071 (1974); R. L. Berger, M. V. Goldman, D .F. DuBois, Phys. Fluids **18**, 207 (1975); J. Weinstock, T. D. Rognlien, and K. F. Lee, Phys. Fluids **18**, 1734 (1975)

[19] V. Yu. Bychenkov, W. Rozmus, A. V. Brantov, and V. T. Tikhonchuk, Phys. Plasmas **7**, 1511 (2000).

[20] V. Yu. Bychenkov, J. Myatt, W. Rozmus, and V. T. Tikhonchuk, PRE **52**, 6759 (1995).

[21] A. Schmitt and B. B. Afeyan, Phys. Plasmas **5** , 503 (1998)

[22] C. H. Still, R. L. Berger, A. B. Langdon, D. E. Hinkel, L. J. Suter, and E. A. Williams, Phys. Plasmas **7**, 2023 (2000).

External Distribution

Plasma Research Laboratory, Australian National University, Australia

Professor I.R. Jones, Flinders University, Australia

Professor João Canalle, Instituto de Fisica DEQ/IF - UERJ, Brazil

Mr. Gerson O. Ludwig, Instituto Nacional de Pesquisas, Brazil

Dr. P.H. Sakanaka, Instituto Fisica, Brazil

The Librarian, Culham Science Center, England

Mrs. S.A. Hutchinson, JET Library, England

Professor M.N. Bussac, Ecole Polytechnique, France

Librarian, Max-Planck-Institut für Plasmaphysik, Germany

Jolan Moldvai, Reports Library, Hungarian Academy of Sciences, Central Research Institute for Physics, Hungary

Dr. P. Kaw, Institute for Plasma Research, India

Ms. P.J. Pathak, Librarian, Institute for Plasma Research, India

Dr. Pandji Triadyaksa, Fakultas MIPA Universitas Diponegoro, Indonesia

Professor Sami Cuperman, Plasma Physics Group, Tel Aviv University, Israel

Ms. Clelia De Palo, Associazione EURATOM-ENEA, Italy

Dr. G. Grosso, Instituto di Fisica del Plasma, Italy

Librarian, Naka Fusion Research Establishment, JAERI, Japan

Library, Laboratory for Complex Energy Processes, Institute for Advanced Study, Kyoto University, Japan

Research Information Center, National Institute for Fusion Science, Japan

Dr. O. Mitarai, Kyushu Tokai University, Japan

Dr. Jiangang Li, Institute of Plasma Physics, Chinese Academy of Sciences, People's Republic of China

Professor Yuping Huo, School of Physical Science and Technology, People's Republic of China

Library, Academia Sinica, Institute of Plasma Physics, People's Republic of China

Librarian, Institute of Physics, Chinese Academy of Sciences, People's Republic of China

Dr. S. Mirnov, TRINITI, Troitsk, Russian Federation, Russia

Dr. V.S. Strelkov, Kurchatov Institute, Russian Federation, Russia

Professor Peter Lukac, Katedra Fyziky Plazmy MFF UK, Mlynska dolina F-2, Komenskeho Univerzita, SK-842 15 Bratislava, Slovakia

Dr. G.S. Lee, Korea Basic Science Institute, South Korea

Dr. Rasulkhozha S. Sharafiddinov, Theoretical Physics Division, Insitute of Nuclear Physics, Uzbekistan

Institute for Plasma Research, University of Maryland, USA

Librarian, Fusion Energy Division, Oak Ridge National Laboratory, USA

Librarian, Institute of Fusion Studies, University of Texas, USA

Librarian, Magnetic Fusion Program, Lawrence Livermore National Laboratory, USA

Library, General Atomics, USA

Plasma Physics Group, Fusion Energy Research Program, University of California at San Diego, USA

Plasma Physics Library, Columbia University, USA

Alkesh Punjabi, Center for Fusion Research and Training, Hampton University, USA

Dr. W.M. Stacey, Fusion Research Center, Georgia Institute of Technology, USA

Dr. John Willis, U.S. Department of Energy, Office of Fusion Energy Sciences, USA

Mr. Paul H. Wright, Indianapolis, Indiana, USA

The Princeton Plasma Physics Laboratory is operated
by Princeton University under contract
with the U.S. Department of Energy.

Information Services
Princeton Plasma Physics Laboratory
P.O. Box 451
Princeton, NJ 08543

Phone: 609-243-2750
Fax: 609-243-2751
e-mail: pppl_info@pppl.gov
Internet Address: http://www.pppl.gov